Spin-glass phase and re-entrant spin-glass phase in diluted three-dimensional Ising antiferromagnet $Ni_cMg_{1-c}(OH)_2$

2000 J. Phys.: Condens. Matter 12 1377

(http://iopscience.iop.org/0953-8984/12/7/320)

J. Phys.: Condens. Matter **12** (2000) 1377–1397. Printed in the UK PII: S0953-8984(00)08801-9

Spin-glass phase and re-entrant spin-glass phase in diluted three-dimensional Ising antiferromagnet $Ni_cMg_{1-c}(OH)_2$

Masatsugu Suzuki†, Itsuko S Suzuki† and Toshiaki Enoki‡

† Department of Physics, State University of New York at Binghamton, Binghamton, NY 13902-6016, USA

‡ Department of Chemistry, Tokyo Institute of Technology, Meguro-ku, Tokyo 152-8551, Japan

Received 19 October 1999

Abstract. The magnetic phase diagram of a diluted three-dimensional Ising antiferromagnet $Ni_cMg_{1-c}(OH)_2$ is determined. It consists of a spin-glass phase for $0.1 < c < 0.5$, a re-entrant spin-glass phase for $0.5 \leqslant c \leqslant 0.8$ and an antiferromagnetic phase for $0.5 \leqslant c \leqslant 1$. The dynamic aspect of the spin-glass phase and the re-entrant spin-glass phase is studied from the temperature, frequency and field dependence of dispersion χ' and absorption χ''. The relaxation time for $c = 0.25$ and 0.8 diverges in accordance with a critical slowing down with a dynamic critical exponent $x = 8.79 \pm 2.44$ for $c = 0.25$ and 10.1 ± 1.3 for $c = 0.8$. The re-entrant spin-glass phase at $c = 0.5$ and 0.6 may be a mixed phase of spin-glass phase and antiferromagnetic phase. The competition between ferromagnetic intraplanar and antiferromagnetic interplanar exchange interaction gives rise to spin-glass behaviour.

1. Introduction

Pure $Ni(OH)_2$ has a CdI_2-type hexagonal structure (space group $C\bar{3}m$). In figure 1 we show the crystalline and magnetic structure of $Ni(OH)_2$. Ni^{2+} ions form a triangular lattice with a lattice constant $a = 3.117$ Å in the c plane. The separation distance between adjacent Ni^{2+} layers is $c = 4.595$ Å. The antiferromagnetic interplanar exchange interactions (J_2 and J_3) are weaker than the ferromagnetic intraplanar exchange interaction (J_1). Because of a negative uniaxial single ion anisotropy D ($= -0.8$ K) magnetic moments of Ni^{2+} spin ($S = 1$) are directed along the c axis. $Ni(OH)_2$ undergoes an antiferromagnetic phase transition at the Néel temperature T_N ($= 26.4$ K). Below T_N the 2D ferromagnetic long range order is established in each Ni^{2+} layer. Such 2D ferromagnetic layers are antiferromagnetically coupled along the c axis, forming a three-dimensional (3D) antiferromagnetic order.

Dilution with Mg^{2+} ions to produce $Ni_cMg_{1-c}(OH)_2$ causes it to behave magnetically like a 3D Ising random spin system. The magnetic properties of $Ni_cMg_{1-c}(OH)_2$ have been studied by Enoki and Tsujikawa [1–3] and Enoki *et al* [4] using DC and AC magnetic susceptibility, and magnetization. The critical temperature T_c decreases with decreasing concentration c for $c > 0.4$. The percolation threshold c_p where T_c reduces to zero is about 0.1. The curve of T_c against c shows a terraced form in the concentration region below $c \approx 0.4$: T_N is extrapolated to zero near $c = 0.33$. Enoki and Tsujikawa [3] have also pointed out that the absorption χ'' for the system with $c < 0.35$ begins to increase as the temperature decreases below T_c: χ'' tends to saturate just below T_c for $0.25 < c < 0.35$, while it continues to increase with decreasing T below T_c for $0.1 < c < 0.17$. Enoki and Tsujikawa [3] have claimed that the occurrence of a χ'' anomaly below $c = 0.35$ may result from possible ferromagnetic short range order.

0953-8984/00/071377+21$30.00

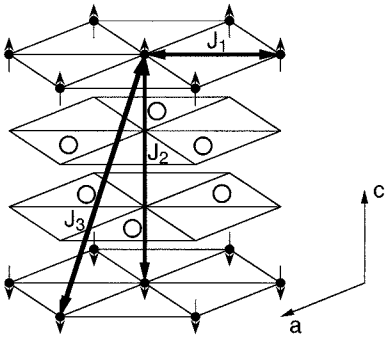

Figure 1. Crystal and magnetic structure of $Ni(OH)_2$. Ni^{2+} (●) and O^{2-} (○). Hydrogen atoms are not shown. $a = 3.117$ Å and $c = 4.595$ Å. $J_1 = 2.7$ K, $J_2 = -0.28$ K, and $J_3 = -0.09$ K.

There has been no report on the frequency dependence of the anomaly of χ'' for $c \leqslant 0.35$. In spite of such work it seems that the magnetic phase transition of this system is not completely understood.

In this paper we have undertaken an extensive study on the magnetic phase transition of $Ni_cMg_{1-c}(OH)_2$ with $0.1 \leqslant c \leqslant 1$ using SQUID DC magnetization and SQUID AC magnetic susceptibility. The magnetic phase diagram presented here is rather different from that reported by Enoki and Tsujikawa [2]. For $0.1 < c < 0.5$ a spin-glass (SG) phase occurs below a critical temperature T_{SG}. For $0.5 \leqslant c \leqslant 0.8$ there are two phase transitions: one from a paramagnetic (P) phase to an antiferromagnetic (AF) phase at a critical temperature T_N and the other from the AF phase to a re-entrant spin-glass (RSG) phase at T_{RSG}. For $c > 0.8$ only the AF phase occurs below T_N.

An irreversible effect of magnetization for SG and RSG phases is examined from the measurements of zero-field cooled (ZFC) and field-cooled (FC) magnetization. The dynamic aspect of the SG and RSG phases is examined from the frequency dependence of χ' and χ''. The magnetic properties of $Ni_cMg_{1-c}(OH)_2$ thus obtained are compared with that of the dilute 3D Ising antiferromagnet $Fe_cMg_{1-c}Cl_2$ [5–8], the 3D Ising short-range spin glass $Fe_cMn_{1-c}TiO_3$ [9, 10] and the quasi-2D XY-like short-range spin-glass stage-2 $Cu_cCo_{1-c}Cl_2$ graphite intercalation compounds (GICs) [11, 12], where the existence of AF phase, SG phase and RSG phase is confirmed.

In the strict sense $Ni_cMg_{1-c}(OH)_2$ magnetically behaves like a 3D Heisenberg short-range spin glass with small Ising symmetry. The Ising character of the spin-glass phase transition may be ascribed to that of a chiral-glass transition. The present work is motivated in part by a theoretical prediction proposed by Kawamura [13]. For the 3D Heisenberg system one may define a local scalar chirality for three neighbouring spins (spin triad) at the i, j and kth sites by $\chi_{ijk} = S_i \cdot (S_j \times S_k)$. The chirality χ_{ijk} is a pseudoscalar in the sense that it is invariant under global SO(3) proper spin rotations while it changes sign under global Z_2 spin reflections or spin inversions. Monte Carlo results [13] show that an isotropic Heisenberg spin glass exhibits a chiral-glass transition at a finite temperature. The universality class of the chiral-glass transition is that of the 3D Ising spin glass. In the presence of random magnetic anisotropy, the symmetry of the Hamiltonian is reduced from $O(3) = Z_2 \times SO(3)$ to Z_2. Since the chiral Z_2 part remains intact in the Hamiltonian, the chiral-glass transition is present even in the presence of weak magnetic anisotropy. However, because of the absence of the SO(3) symmetry in the Hamiltonian, the Heisenberg spin is now not allowed to remain disordered once the chiral-glass transition takes place. It is forced to order by chirality, leading to the mixing of the spin and chirality which are separated by symmetry in a fully isotropic case. Then the chiral-glass transition, which is hidden in the chirality in the absence of magnetic

anisotropy, might manifest itself in the divergence of the conventional spin-glass susceptibility through the coupling between the spin and chirality generated by the weak magnetic anisotropy.

2. Experimental procedure

Powdered samples of $Ni_cMg_{1-c}(OH)_2$ used in the present work were the same as those used in the previous work by Enoki and Tsujikawa [1–3]. The details of sample preparation were reported in [1]. The DC magnetization and AC magnetic susceptibility of $Ni_cMg_{1-c}(OH)_2$ with $c = 0.1$, 0.25, 0.315, 0.5, 0.6, 0.8 and 1 were measured using a SQUID magnetometer (Quantum Design, MPMS XL-5) with an ultra-low-field capability option.

(i) *DC magnetization*. Before setting up a sample at 298 K, a remanent magnetic field in a superconducting magnet was reduced to one less than 3 mOe using an ultra-low-field capability option. For convenience, hereafter this remanent field is noted as the state of $H = 0$. The sample was cooled from 298 K to 1.9 K at $H = 0$. Then an external magnetic field H was applied at 1.9 K. The zero-field-cooled magnetization (M_{ZFC}) was measured with increasing T from 1.9 K to a certain temperature T_0 which is different for each concentration. After that the sample was kept at 60 K for 20 minutes and again cooled to T_0 in the presence of the same field H. Then the field-cooled magnetization (M_{FC}) was measured with decreasing T from a temperature T_0 to 1.9 K.

(ii) *AC magnetic susceptibility in $H = 0$.* A sample was cooled from 298 K to 1.9 K at $H = 0$. Then both χ' and χ'' were simultaneously measured as a function of frequency (0.01 Hz $\leqslant f \leqslant$ 1000 Hz) at fixed T, where T was increased from 1.9 K to T_0 after each frequency scan. The amplitude of AC magnetic field h is kept as low as possible: $h = 0.1$ Oe, 0.5 Oe and 1 Oe.

(iii) *AC magnetic susceptibility in $H \neq 0$.* A sample was cooled from 298 K to 1.9 K in $H = 0$. Then both χ' and χ'' at a fixed frequency ($f = 1$ Hz) were simultaneously measured as a function of T in the presence of fixed H. The data were taken when T was increased from 1.9 K to T_0. The magnetic field H was changed after each T scan.

3. Result

3.1. $c = 0.1$

The T dependence of χ_{FC} ($= M_{FC}/H$) and χ_{ZFC} ($= M_{ZFC}/H$) for $c = 0.1$ was measured in the presence of $H = 1$ Oe. Both χ_{FC} and χ_{ZFC} decrease with increasing T. The difference δ ($= \chi_{FC} - \chi_{ZFC}$) drastically increases with decreasing T and exhibits a sharp peak at 2.2 K. The T dependence of χ' and χ'' for $c = 0.1$ was also measured at various f ($0.01 \leqslant f \leqslant 1000$ Hz), where $h = 0.5$ Oe. The dispersion χ' increases with decreasing T for $0.01 \leqslant f \leqslant 200$ Hz. It exhibits a broad peak around 2.05 K at $f = 330$ Hz, which slightly shifts to the high temperature side with increasing f. In contrast, χ'' starts to appear below $\approx$3 K and increases with decreasing T. The increase of χ'' with decreasing T below 2.1 K becomes more remarkable as f increases.

3.2. $c = 0.25$ and 0.315

Figure 2 shows the T dependence of χ_{FC}, χ_{ZFC}, and δ for $c = 0.25$, where $H = 1$ Oe. The susceptibility χ_{ZFC} has a broad peak at 2.3 K, while χ_{FC} increases with decreasing T. The difference δ is almost zero above 3.5 K. It begins to appear below 2.7 K and dramatically increases with decreasing T below 2.3 K. The irreversible effect of magnetization clearly

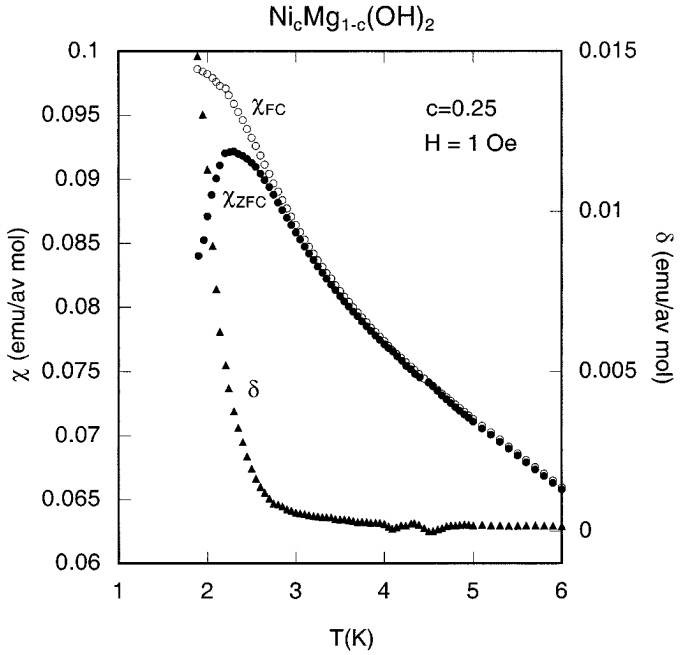

Figure 2. T dependence of χ_{FC} ($= M_{FC}/H$) (○), χ_{ZFC}($= M_{ZFC}/H$) (●), and δ ($= \chi_{FC} - \chi_{ZFC}$) (▲) for $Ni_cMg_{1-c}(OH)_2$ with $c = 0.25$. $H = 1$ Oe.

indicates the occurrence of spin-glass behaviour. Figures 3(a) and (b) show the T dependence of χ' and χ'' for $c = 0.25$ at various f, respectively, where $h = 0.5$ Oe. In figure 3(a) χ' exhibits a peak at 2.5 K for $f = 0.01$ Hz, which is defined as T_{SG} for $c = 0.25$. This peak shifts to the high temperature side with increasing f: 3.15 K at $f = 1$ kHz. In figure 3(b) χ'' increases with decreasing T for $0.01 \leqslant f \leqslant 0.2$ Hz. It exhibits a peak at 2.1 K for $f = 0.3$ Hz, shifting to the high temperature side with increasing f: 2.3 K for $f = 1$ kHz. Figure 4 shows the T dependence of χ'' for $c = 0.25$ for various H, where $f = 1$ Hz and $h = 0.5$ Oe. The peak at 2.1 K for $H = 0$ shifts to the low temperature side with increasing H. We find that a characteristic temperature T^0_{SG} at which χ'' reduces to zero is rather higher than T_{SG} (= 2.5 K). The value of T^0_{SG} decreases with increasing H. The H dependence of T^0_{SG} will be discussed in section 4.2.

The T and f dependence of χ' and χ'' for $c = 0.315$ was also examined. These results are almost the same as those obtained for $c = 0.25$. The dispersion χ' at $f = 0.01$ Hz exhibits a peak at T_{SG}(= 2.5 K), while χ_{ZFC} shows a peak at 2.3 K.

3.3. c = 0.5

Figure 5 shows the T dependence of χ_{FC}, χ_{ZFC}, and δ for $c = 0.5$ in the presence of $H = 1$ Oe. Both χ_{ZFC} and χ_{FC} show a peak: the peak temperature for χ_{FC} (= 10.1 K) is slightly lower than that for χ_{ZFC} (= 10.2 K). This peak clearly indicates that there occurs a transition between the P phase and the AF phase at T_N. Note that T_N (defined as a temperature where a derivative T ($\mathrm{d}\chi_{FC}/\mathrm{d}T$) has a maximum) is a little lower than the peak temperature of χ_{FC}. For convenience hereafter we define the peak temperature of χ_{FC} as T_N (= 10.1 K). The difference δ for $c = 0.5$ begins to appear around 12 K higher than T_N. It shows a plateau-like

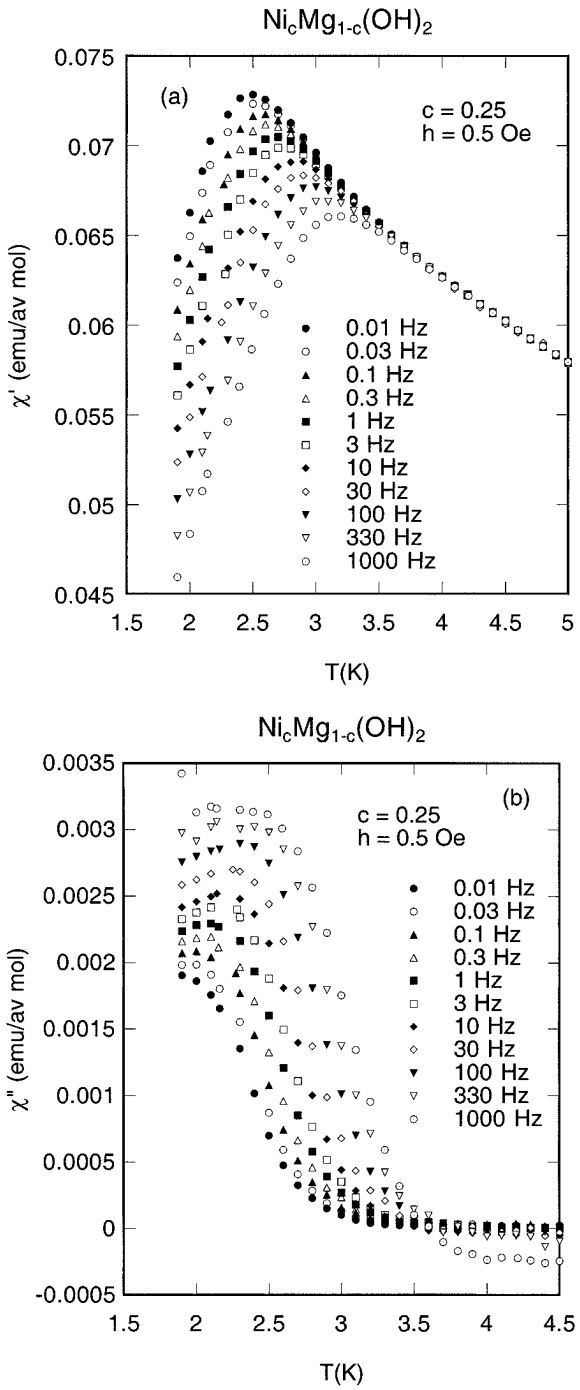

Figure 3. T dependence of (a) χ' and (b) χ'' for $c = 0.25$ with various f. $h = 0.5$ Oe. $H = 0$.

behaviour below T_N and dramatically increases below 5.3 K with decreasing T, suggesting the occurrence of a transition between the AF phase and the RSG phase around 5.3 K. In figure 5 we also show the T dependence of χ' for $c = 0.5$ where $H = 0$, $f = 1.0$ Hz and $h = 0.1$ Oe.

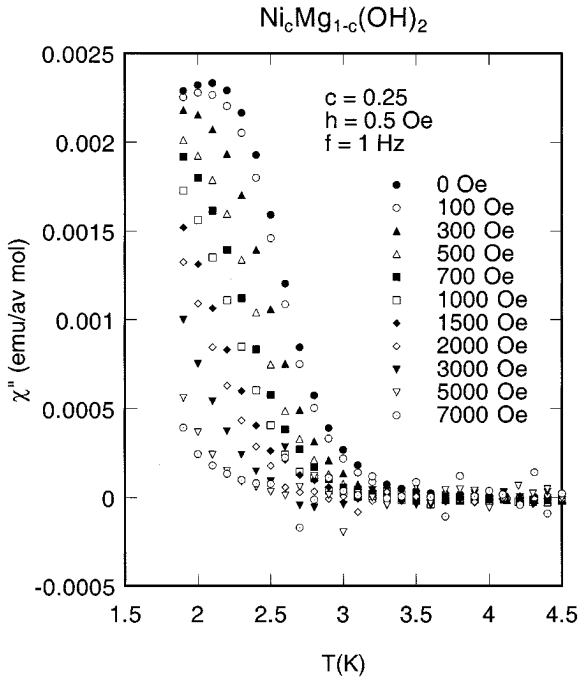

Figure 4. T dependence of χ'' for $c = 0.25$ at various H. $h = 0.5$ Oe. $f = 1$ Hz.

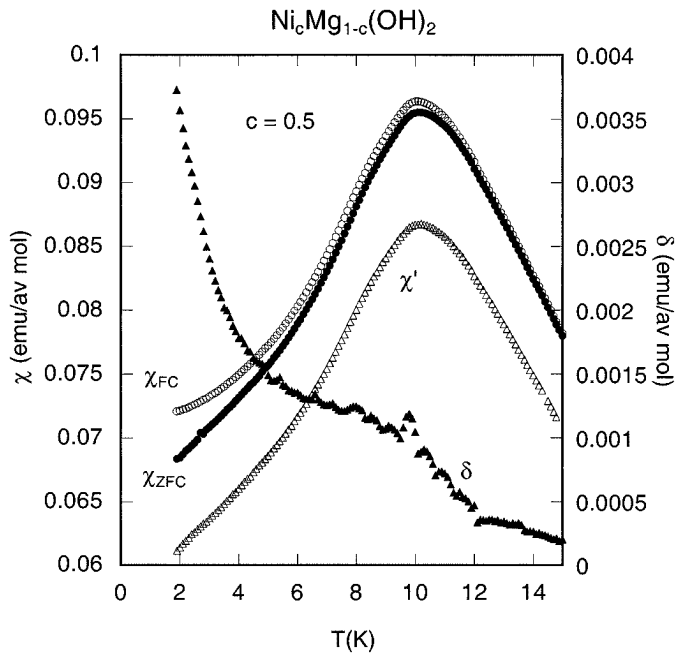

Figure 5. T dependence of χ_{FC} (○), χ_{ZFC} (●), δ (▲), and χ' (△) for $c = 0.5$, where χ_{FC} and χ_{ZFC} were measured in the presence of $H = 1$ Oe and χ' was measured at $f = 1$ Hz and $h = 0.1$ Oe. $H = 0$.

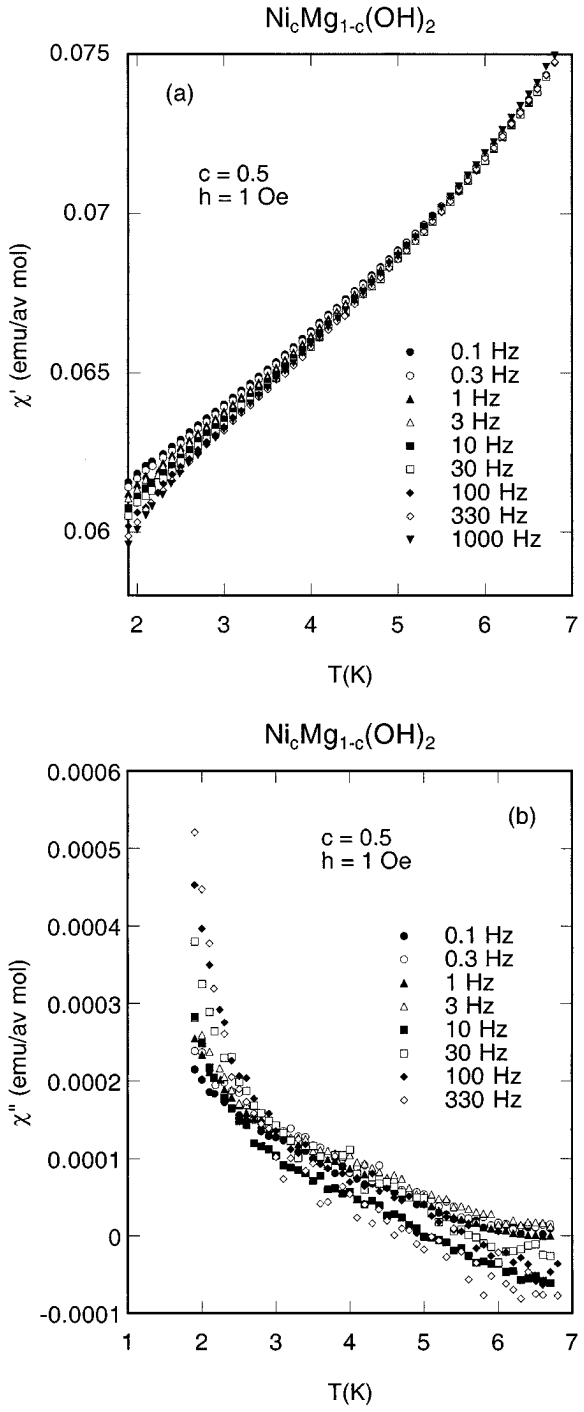

Figure 6. T dependence of (a) χ' and (b) χ'' for $c = 0.5$ at various f. $h = 1$ Oe. $H = 0$.

The T dependence of χ' is similar to that of χ_{ZFC}, except for a constant term: χ' has a peak at 10.2 K.

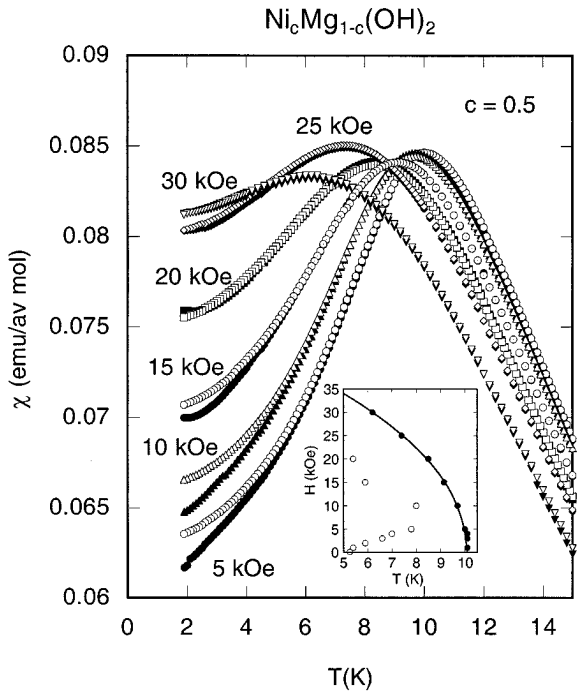

Figure 7. T dependence of χ_{FC} (○) and χ_{ZFC} (●) for $c = 0.5$ at various H (= 5–30 kOe). The inset shows the magnetic phase diagram of H against T_N (●) and H against T^0_{RSG} (○). The solid line denotes a least-squares fitting curve for H against T_N (see the text).

Figures 6(a) and (b) show the T dependence of χ' and χ'' for $c = 0.5$ at various f, respectively, where $h = 1$ Oe. The dispersion χ' is almost independent of f above 6 K. It becomes gradually dependent on f with decreasing T:χ' decreases with increasing f at fixed T below 6 K. The absorption χ'' for each f decreases with increasing T and reduces to zero around 6 K. We define a temperature at which χ'' at $f = 0.1$ Hz reduces to zero as T_{RSG}(= 6.0 K) for $c = 0.5$.

Figure 7 shows the T dependence of χ_{FC} and χ_{ZFC} for $c = 0.5$ at various H. The Néel temperature T_N decreases with increasing H. The inset of figure 7 shows the H dependence of T_N: The least squares fit of data to $H = H_0[1 - T_N(H)/T_N(H = 0)]^{\mu}$ yields parameters $\mu = 0.47 \pm 0.02$, $T_N(H = 0) = 10.08 \pm 0.05$ K and $H_0 = 47 \pm 3$ kOe. The difference δ ($= \chi_{FC} - \chi_{ZFC}$) drastically increases below a characteristic temperature T^0_{RSG} below T_N for $H \leqslant 20$ kOe. In the inset of figure 7 we also show the H dependence of T^0_{RSG}. It increases with increasing H and reaches a maximum at $H \approx 10$ kOe which is much lower than the corresponding T_N. It decreases with further increasing H for $10 \leqslant H \leqslant 20$ kOe. Similar behaviour has been observed in $Fe_cMg_{1-c}Cl_2$ with $c = 0.552$ by Gelard *et al* [6].

3.4. c = 0.6

Figure 8 shows the T dependence of χ_{FC}, χ_{ZFC} and δ for $c = 0.6$ in the presence of $H = 1$ Oe. The susceptibility χ_{FC} and χ_{ZFC} exhibit a peak at T_N (= 13.8 K) and 13.9 K, respectively. The difference δ appears below 18.9 K higher than T_N. It shows a plateau-like behaviour below T_N and dramatically increases with decreasing T below 3.1 K.

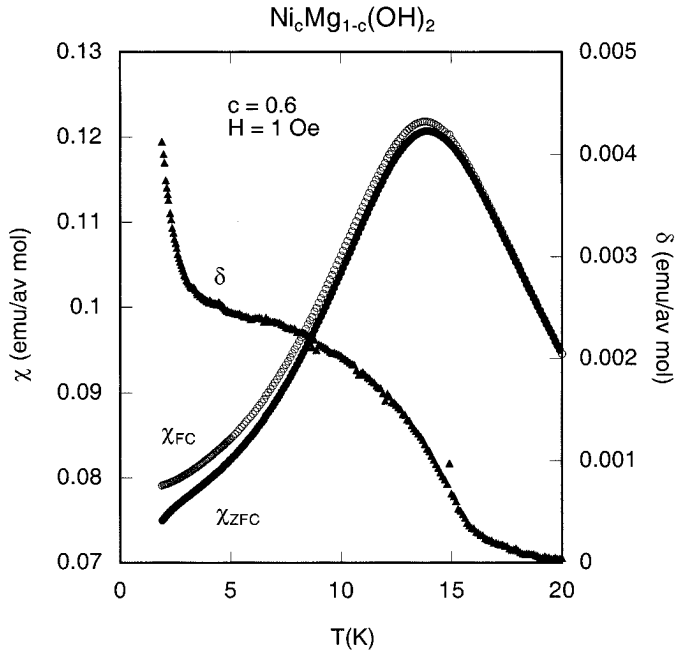

Figure 8. T dependence of χ_{FC} (○), χ_{ZFC} (●), and δ (▲) for $c = 0.6$. $H = 1$ Oe.

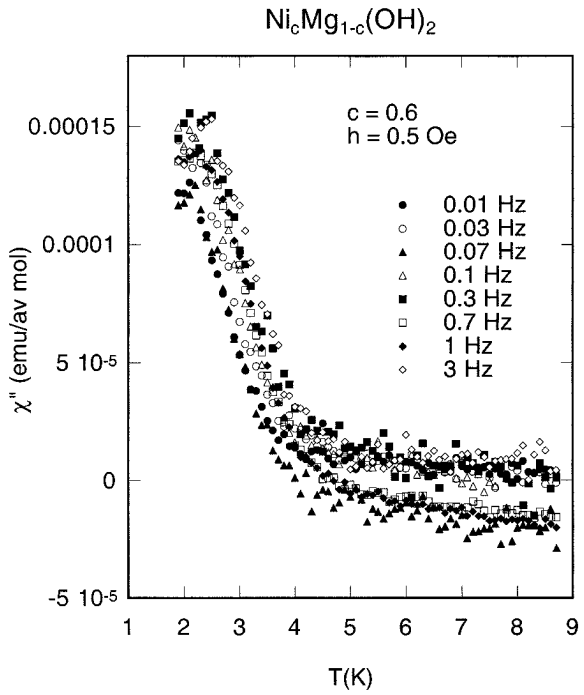

Figure 9. T dependence of χ'' for $c = 0.6$ with various f. $h = 0.5$ Oe. $H = 0$.

Figure 9 shows the T dependence of χ'' for $c = 0.6$ at various f, where $h = 0.5$ Oe. The absorption χ'' for each f decreases with increasing T and reduces to zero around 4.5 K.

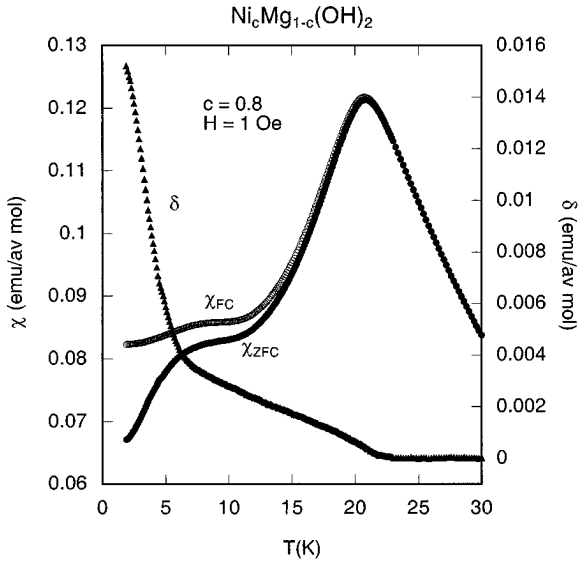

Figure 10. T dependence of χ_{FC} (○), χ_{ZFC} (●), and δ (▲) for $c = 0.8$. $H = 1$ Oe.

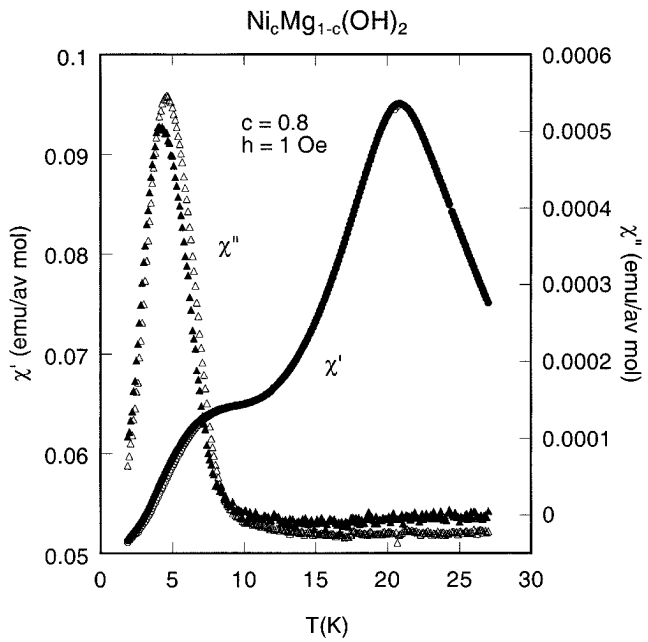

Figure 11. T dependence of χ' and χ'' for $c = 0.8$ at $f = 0.1$ and 1 Hz. $h = 1$ Oe. $H = 0$. χ' (0.1 Hz) (●), χ' (1 Hz) (○), χ'' (0.1 Hz) (▲), and χ'' (1 Hz) (△).

We define a temperature at which χ'' at $f = 0.01$ Hz reduces to zero, as T_{RSG} (= 4.5 K) for $c = 0.6$: T_{RSG} seems to increase with increasing f from figure 9.

3.5. c = 0.8

Figure 10 shows the T dependence of χ_{FC}, χ_{ZFC}, and δ for $c = 0.8$ in the presence of $H = 1$ Oe : χ_{FC} has a small peak around 8.6 K and a broad peak at T_N (= 20.7 K), while

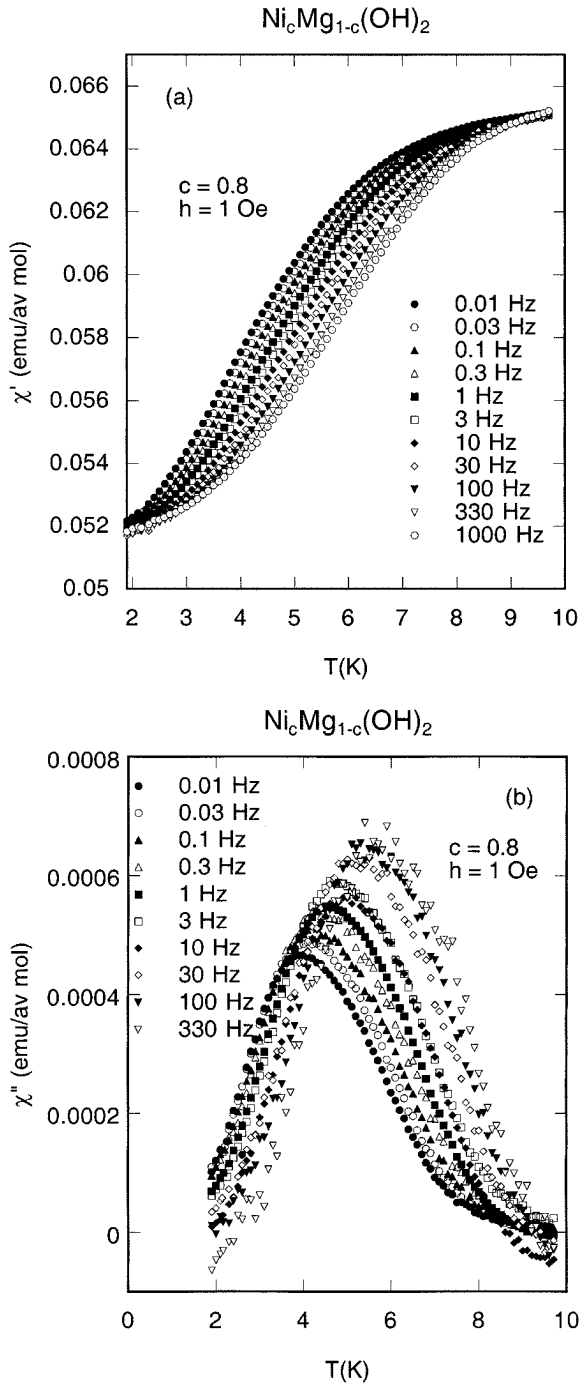

Figure 12. T dependence of (a) χ' and (b) χ'' for $c = 0.8$ at various f. $h = 1$ Oe. $H = 0$.

χ_{ZFC} has a broad shoulder around 6-8 K and a peak at 20.8 K. The difference δ begins to appear around 23.3 K. It linearly increases with decreasing T below T_N and dramatically

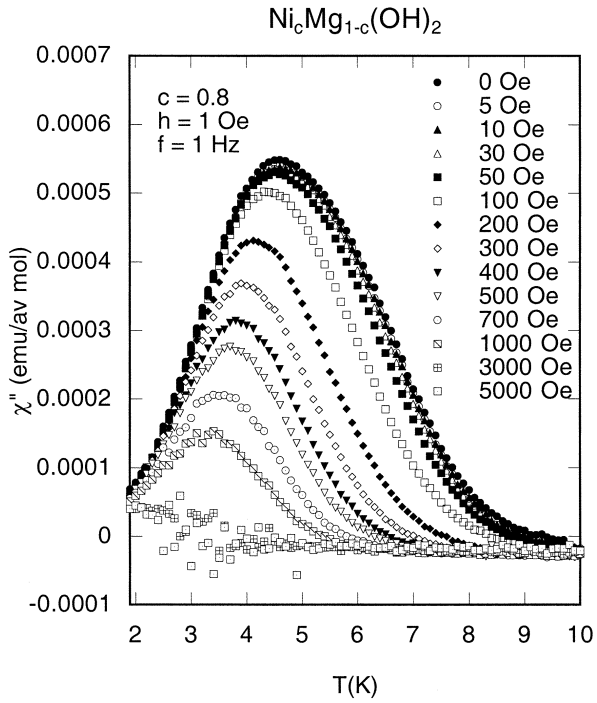

Figure 13. T dependence of χ'' for $c = 0.8$ at various H. $h = 1$ Oe. $f = 1$ Hz.

increases below 4.3 K. Figure 11 shows the T dependence of χ' and χ'' at $f = 0.1$ and 1 Hz for $1.9 \leqslant T \leqslant 30$ K, where $h = 1$ Oe. The absorption χ'' has a sharp peak at 4.2 K for $f = 0.1$ Hz and 4.55 K for $f = 1$ Hz. No anomaly in χ'' is observed above these temperatures. The T dependence of χ' is similar to that of χ_{ZFC}: a broad shoulder around 6–8 K and a peak at 20.8 K. Figures 12(a) and (b) show the T dependence of χ' and χ'' for $c = 0.8$ at various f for $1.9 \leqslant T \leqslant 9.5$ K, where $h = 1$ Oe. The absorption χ'' shows a peak at T_{RSG} (= 4.0 K) at $f = 0.01$ Hz, shifting to the high temperature side with increasing f. These results indicate that the transition occurs between the AF phase and RSG phase at T_{RSG}. In contrast, the dispersion χ' shows a shoulder around 5–6 K, which is strongly dependent on f. Figure 13 shows the T dependence of χ'' for $c = 0.8$ at various H, where $f = 1$ Hz and $h = 1$ Oe. The absorption χ'' has a peak at 4.59 K for $H = 0$, shifting to the low temperature side with increasing H. The H dependence of the peak temperature corresponding to $T_{RSG}(H)$ will be discussed in section 4.2.

3.6. c = 1

Figure 14 shows the T dependence of χ_{FC}, χ_{ZFC}, and δ for $c = 1$ in the presence of $H = 1$ Oe. Both χ_{FC} and χ_{ZFC}, have a sharp peak at T_N (= 26.4 K) and 26.5 K, respectively. The difference δ appears below 27.1 K just above T_N, showing a small peak at 26.2 K, and increases with further decreasing T. No abrupt increase in δ is observed at low T, suggesting the absence of spin-glass behaviour.

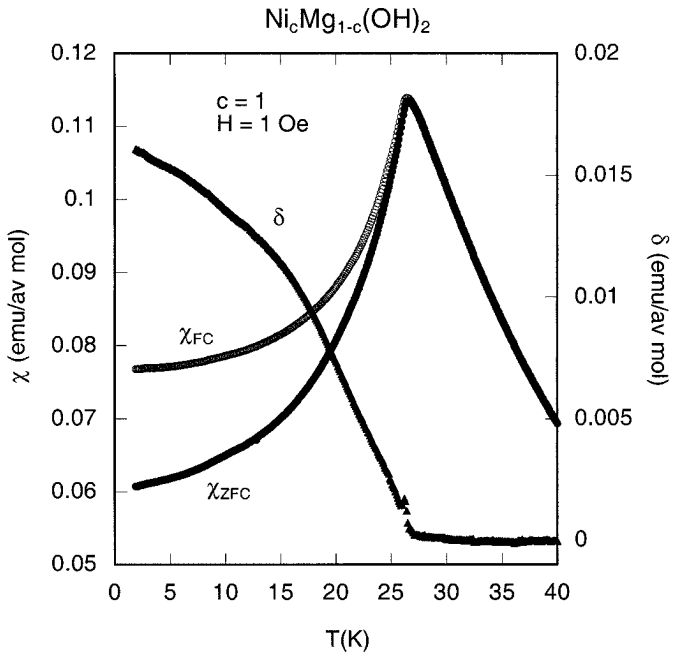

Figure 14. T dependence of χ_{FC} (○). χ_{ZFC} (●), and δ (▲) for $c = 1$. $H = 1$ Oe.

4. Discussion

4.1. Magnetic phase diagram

Figure 15 shows the magnetic phase diagram of the critical temperature against c for $Ni_cMg_{1-c}(OH)_2$. For comparison the data obtained by Enoki and Tsujikawa [2] are denoted by open circles. For $0.1 < c < 0.5$ the system undergoes a transition between the P phase and SG phase at T_{SG}. The temperature T_{SG} for $c = 0.2$ and 0.315 is defined as a temperature where χ' shows a peak at $f = 0.01$ Hz: $T_{SG} = 5$ K for both $c = 0.2$ and 0.315 denoted by closed squares in figure 15. For $0.5 \leqslant c \leqslant 0.8$ the system undergoes two transitions: one between the P phase and AF phase at T_N and the other between the AF phase and RSG phase at T_{RSG}. The temperature T_{RSG} for $c = 0.5$ and 0.6 is defined as a temperature at which χ'' at $f = 0.1$ or 0.01 Hz reduces to zero, while T_{RSG} for $c = 0.8$ is defined as a temperature at which χ'' at $f = 0.01$ Hz shows a peak: $T_{RSG} = 6$ K for $c = 0.5$, 4.5 K for $c = 0.6$ and 4.0 K for $c = 0.8$ denoted by closed triangles. The Néel temperature T_N is defined as a temperature at which χ_{FC} has a peak: $T_N = 10.1$ K for $c = 0.5$, 13.8 K for $c = 0.6$ and 20.7 K for $c = 0.8$ denoted by closed circles. For $c > 0.8$ the system undergoes a transition between the P phase and AF phase at T_N:$T_N = 26.4$ K for $c = 1$. In figure 15 it seems that the point at $c \approx 0.45$ and $T \approx 6.6$ K is the multicritical point, where the SG, RSG and AF phases merge. The P to AF phase transition line appears to be linear with a slope $\mathrm{d}(T_N(c)/T_N(c=1))/\mathrm{d}c = 1.24 \pm 0.05$ using our data of T_N against c for $0.5 \leqslant c \leqslant 1$.

4.2. Nature of SG phase ($c = 0.25$) and RSG phase ($c = 0.8$)

Figures 16(a) and (b) show the f dependence of χ' and χ'' for $c = 0.25$ at various T, respectively, for $0.01 \leqslant f \leqslant 1000$ Hz. The dispersion χ' is almost independent of f above

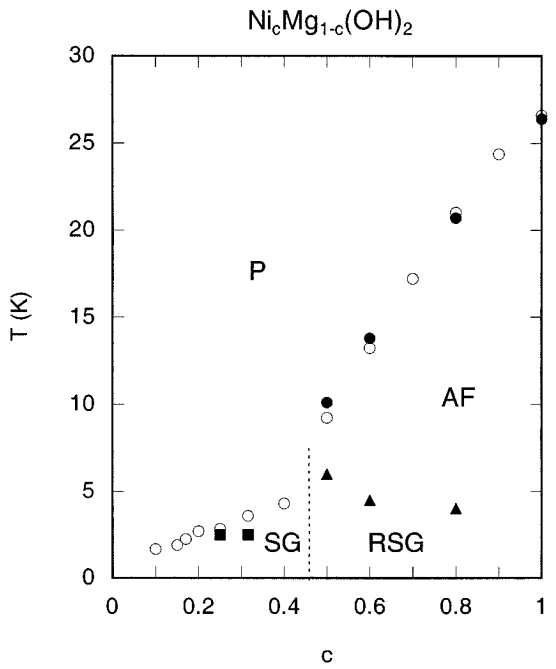

Figure 15. Magnetic phase diagram (critical temperature against Ni concentration c) of $Ni_cMg_{1-c}(OH)_2$. P: paramagnetic phase, AF: antiferromagnetic phase, SG: spin-glass phase, RSG: re-entrant spin-glass phase. The data reported by Enoki and Tsujikawa [2] are denoted by open circles.

3.3 K, while χ' dramatically decreases with increasing f below T_{SG} (= 2.5 K). In contrast χ'' increases with increasing f at any T. No peak in χ'' is observed for $0.01 \leqslant f \leqslant 1000$ Hz. Nevertheless, χ'' at frequencies lower than 10 Hz dramatically increases below T_{SG}. This f dependence of χ'' is essentially different from that of systems with a single relaxation time of Debye type, where χ'' has a peak at $\omega\tau = 1$. Figure 16(c) shows the T dependence of the average relaxation time τ for $c = 0.25$ and 0.315, where τ is determined from the assumption that χ' has a peak at $\omega\tau = 1$ in the curve of χ' against T (figure 3(a)). The data for $c = 0.315$ is very similar to those for $c = 0.25$. The average relaxation time τ divergingly increases with decreasing T in such a limited temperature range. The most likely source for such a divergence of τ is a critical slowing down. The relaxation time τ can be described by a power law form

$$\tau = \tau_0(T/T^* - 1)^{-x} \tag{1}$$

where x is a critical exponent, T^* is a finite critical temperature and τ_0 is a characteristic time. The least-squares fit of the data for $c = 0.25$ to (1) for $2.5 \leqslant T \leqslant 3.15$ K yields parameters $x = 8.79 \pm 2.44$, $T^* = 2.25 \pm 0.14$ K, and $\tau_0 = (4.2 \pm 0.8) \times 10^{-8}$ s. Note that $x = 10.0 \pm 1.0$ for the SG phase of a typical 3D Ising short-range spin glass $Fe_{0.5}Mn_{0.5}TiO_3$ [9]. The solid line in figure 16(c) is a least-squares fitting curve thus obtained. The value of T^* is a little lower than T_{SG} (= 2.5 K). The inset of figure 16(c) shows the H dependence of T_{SG}^0 defined in section 3.2. The change of peak temperature $T_{SG}^0(H)$ with H is well described by a relation

$$H = H_0\left[1 - \frac{T_{SG}^0(H)}{T_{SG}^0(H=0)}\right]^{\alpha} \tag{2}$$

with T_{SG}^0 $(H = 0) = 3.60$ K, $H_0 = 8.2 \pm 0.5$ kOe and $\alpha = 2.56 \pm 0.22$. The exponent α is larger than that ($\alpha = 1.5$) predicted by de Almeida and Thouless [14] for the H dependence of freezing temperature at the transition between the P and SG phases. Note that $\alpha = 3.31 \pm 0.54$ for the SG phase of stage-2 $Cu_{0.93}Co_{0.07}Cl_2$ GIC [11, 12]. No reasonable explanation can be given for such large values of α.

Figures 17(a) and (b) show the f dependence of χ' and χ'' for $c = 0.8$ at various T, respectively, for $0.01 \leqslant f \leqslant 1000$ Hz, which is very different from that for $c = 0.25$. The dispersion χ' decreases with increasing f. The f dependence of χ' is described by a power-law form ($\chi' \approx \omega^{-y}$). The least-squares fit of the data to this power-law form for $0.01 \leqslant f \leqslant 1000$ Hz yields the exponent y for each T. The exponent y is dependent on T: it shows a peak ($y = (6.33 \pm 0.09) \times 10^{-3}$) at $T = 4.8$ K a little higher than T_{RSG} (= 4.0 K). The absorption χ'' at 4.0 K exhibits a peak at $f = 0.3$ Hz, shifting to the higher frequency side with increasing T. The absorption χ'' above 6 K increases with f for $0.01 \leqslant f \leqslant 1000$ Hz. These features are common to spin-glass behaviour. Figure 17(c) shows the T dependence of the average relaxation time τ, where τ is determined from the assumption that χ'' has a peak at $\omega\tau = 1$ in the curve of χ'' against T (figure 12(b)). The least-squares fit of the data for $4.0 \leqslant T \leqslant 6.2$ K to (1) yields parameters $x = 10.1 \pm 1.3$, $T^* = 2.87 \pm 0.27$ K and $\tau_0 = (6.9 \pm 1.5) \times 10^{-4}$ s. Note that $x = 13 \pm 2$ for the RSG phase of $Fe_{0.62}Mn_{0.38}TiO_3$ [10]. The solid line in figure 17(c) is a least-squares fitting curve thus obtained. The value of T^* is rather lower than T_{RSG} (= 4.0 K). The inset of figure 17(c) shows the H dependence of T_{RSG} for $c = 0.8$ which is obtained from figure 13. The change of $T_{RSG}(H)$ with H is well described by a relation

$$H = H_0 \left[1 - \frac{T_{RSG}(H)}{T_{RSG}(H = 0)} \right]^{\alpha} \tag{3}$$

with $\alpha = 1.58 \pm 0.15$, T_{RSG} $(H = 0) = 4.59$ K and $H_0 = 7.3 \pm 0.5$ kOe. This value of α is close to that predicted by de Almeida and Thouless [14]. Note that $\alpha = 1.26 \pm 0.02$ for the RSG phase of stage-2 $Cu_{0.8}Co_{0.2}Cl_2$ GIC [11, 12], which is close to that ($\alpha = 1.3$) predicted from the chiral-glass theory [15].

It is interesting to compare our result with theories. Ogielski [16] has predicted from Monte Carlo simulation of a 3D $\pm J$ Ising spin-glass model with short-range interactions that (i) the static properties clearly show a spin-glass ordering transition at a finite freezing temperature $T_f = 1.175\ J$ with the critical exponent of the correlation length $\nu = 1.3$, and that (ii) as T approaches T_f from the high-temperature side a relaxation time τ diverges in accordance with (1) with $x = 7.9 \pm 1.0$, which is unusually large. The value of x for $c = 0.25$ is close to this prediction. The value of x for $c = 0.8$ is larger than this prediction and is close to 10.0 for $Fe_{0.5}Mn_{0.5}TiO_3$ [9]. The values of T^* for $c = 0.25$ and 0.8 are a little lower than T_f (= $1.175J_1 = 3.17$ K) which is calculated by assuming $J = J_1$ (= 2.7 K) for $Ni(OH)_2$ [1]. These results indicate that the spin-glass behaviour at $c = 0.25$ and 0.8 is well described by the 3D Ising short-range spin-glass model. This Ising character may be ascribed to that of the chiral-glass transition predicted by Kawamura [13] for the 3D Heisenberg short-range spin glass with small Ising symmetry.

4.3. Possibility of coexistence in SG and AF phase at c = 0.5 and 0.6

We notice that the T and f dependence of χ' and χ'' for $Ni_cMg_{1-c}(OH)_2$ with $c = 0.5$ and 0.6 is quite similar to that for $Fe_cMg_{1-c}Cl_2$ with $c = 0.55$ ($T_N = 7.5$ K and $T_{RSG} \approx 3$ K) reported by Wong *et al* [8]. They are rather different from those of typical spin glasses where both χ' and χ'' have a peak shifting to the high temperature side with increasing f [17].

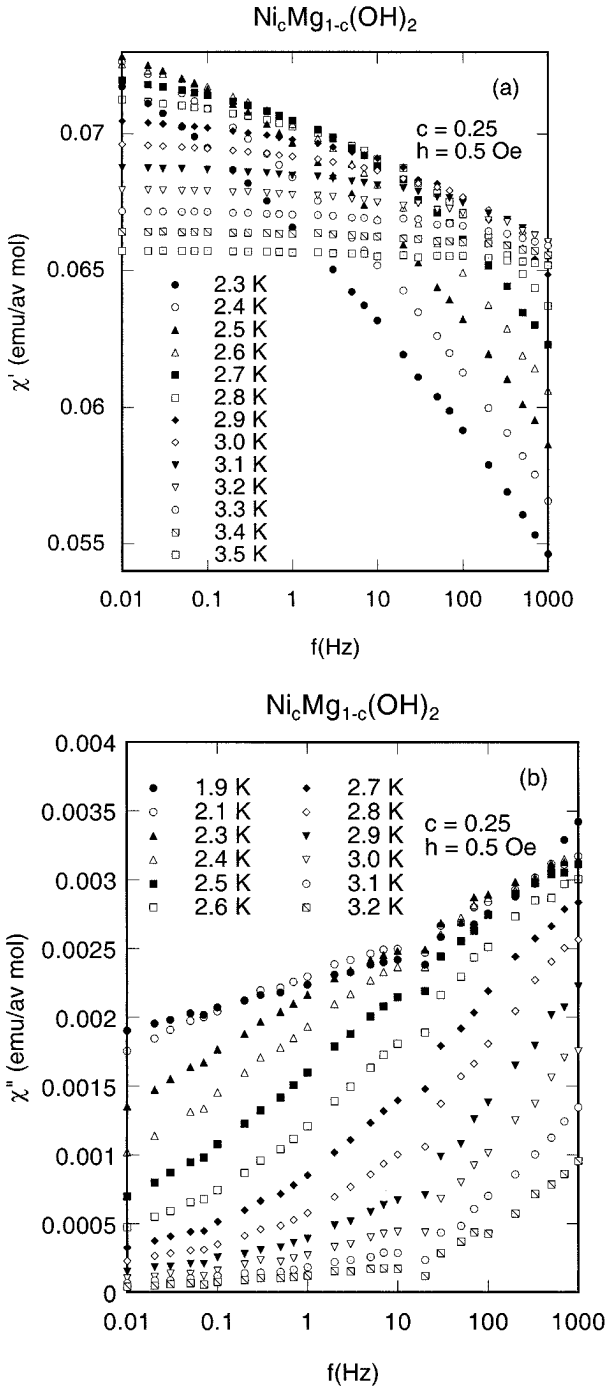

Figure 16. f dependence of (a) χ' and (b) χ'' for $c = 0.25$. $h = 0.5$ Oe. $H = 0$. (c) T dependence of the relaxation time τ for $c = 0.25$ and 0.315, which is determined from the assumption that χ' has a peak at $\omega\tau = 1$ for each f in figure 3(a). The inset shows the H dependence of T_{SG}^0 defined in the text for $c = 0.25$. The solid lines denote least-squares fitting curves for $c = 0.25$ (see the text).

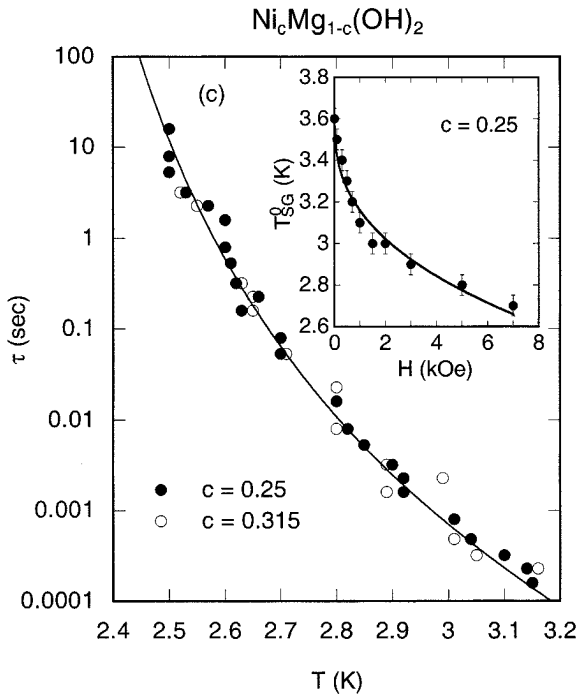

Figure 16. (Continued)

The H dependence of T_{RSG} for $Ni_cMg_{1-c}(OH)_2$ with $c = 0.5$ is also similar to that for $Fe_cMg_{1-c}Cl_2$ with $c = 0.552$ reported by Gelard *et al* [6]. Like a pure $Ni(OH)_2$ a pure $FeCl_2$ magnetically behaves like an Ising antiferromagnet where the direction of spins is along the c axis. It undergoes an antiferromagnetic phase transition at T_N (= 23.55 K), below which the 2D ferromagnetic layers are antiferromagnetically coupled along the c axis. The magnetic neutron scattering study on $Fe_cMg_{1-c}Cl_2$ with $c = 0.55$ by Wong *et al* [8] directly demonstrates that the long-range AF order below T_N is not destroyed by the RSG transition at T_{RSG}. The magnetic Bragg scattering intensity at $(1, 0, \bar{1})$ increases smoothly down to 1.2 K, suggesting that the AF order is not affected by the RSG transition at T_{RSG}. The diffuse scattering intensity at $(0.98, 0, \bar{1})$, which has a peak at T_N because of critical scattering, is much higher than the background at lower T, suggesting that not all the spins are antiferromagnetically ordered. An $(h, 0, \bar{1})$ scan at 1.5 K exhibits a Lorentzian magnetic diffuse peak under the Bragg peak at $(1, 0, \bar{1})$. The width of this peak corresponds to a correlation length ξ of approximately 10 Å. Thus it is concluded that the low-temperature phase below T_{RSG} consists of both SG and long-range AF order. Such a frozen short-range spin correlation may be the origin of the RSG phase observed in χ' and χ'' of $Ni_cMg_{1-c}(OH)_2$ for $c = 0.5$ and 0.6. In spite of the lack of magnetic neutron scattering data, it is concluded from such a similarity in χ' and χ'' that the coexistence of SG and AF order may occur below T_{RSG} in $Ni_cMg_{1-c}(OH)_2$ for $c = 0.5$ and 0.6. The system may consist of majority spins on an infinite AF network and minority spins frozen like a spin glass.

This RSG phase at $c = 0.5$ is affected by the presence of a uniform H: the critical temperature $T_{RSG}(H)$ increases with increasing H below 10 kOe. This behaviour can be qualitatively explained in terms of the random field effect [18]. For a 3D diluted Ising

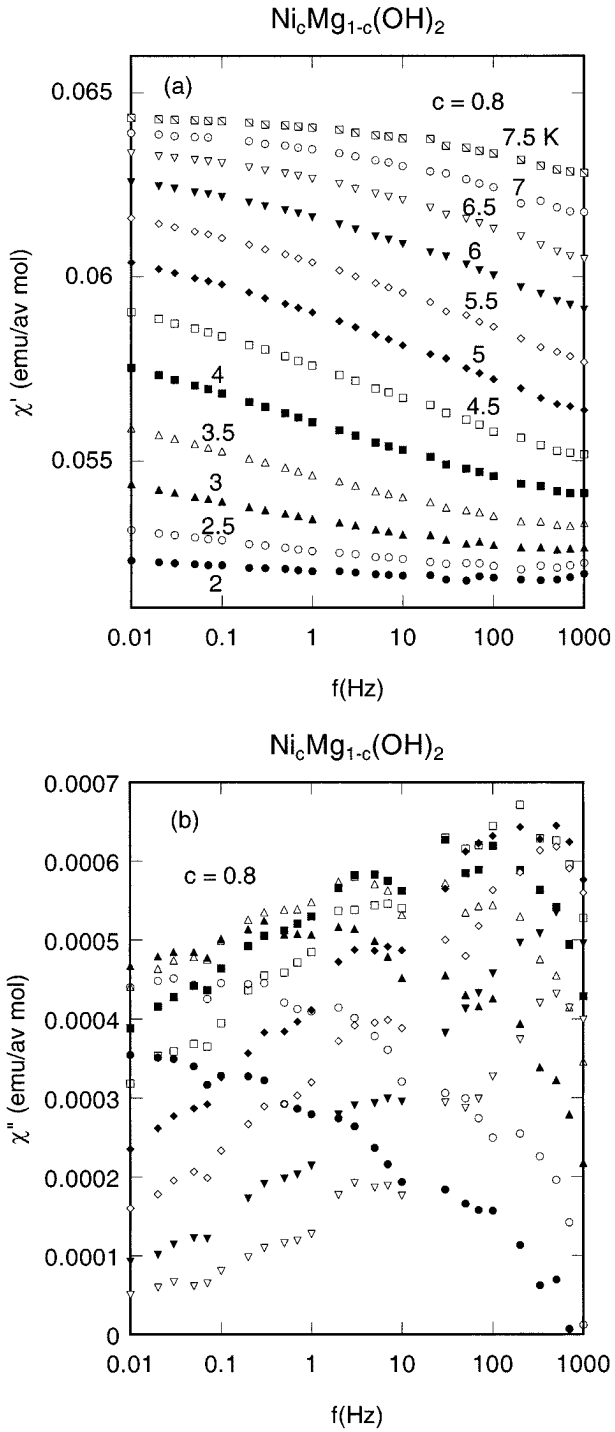

Figure 17. f dependence of (a) χ' and (b) χ'' for $c = 0.8$. $h = 1$ Oe. $H = 0$. For (b) $T = 3$ (●), 3.5 (○), 4 (▲), 4.5 (△), 5 (■), 5.5 (□), 6 (◆), 6.5 (◇), 7 (▼), and 7.5 K (▽). (c) T dependence of the relaxation time τ for $c = 0.8$, which is determined from the assumption that χ'' has a peak at $\omega\tau = 1$ for each f in figure 12(b). The inset shows the H dependence of T_{RSG}. The solid lines denote least-squares fitting curves (see the text).

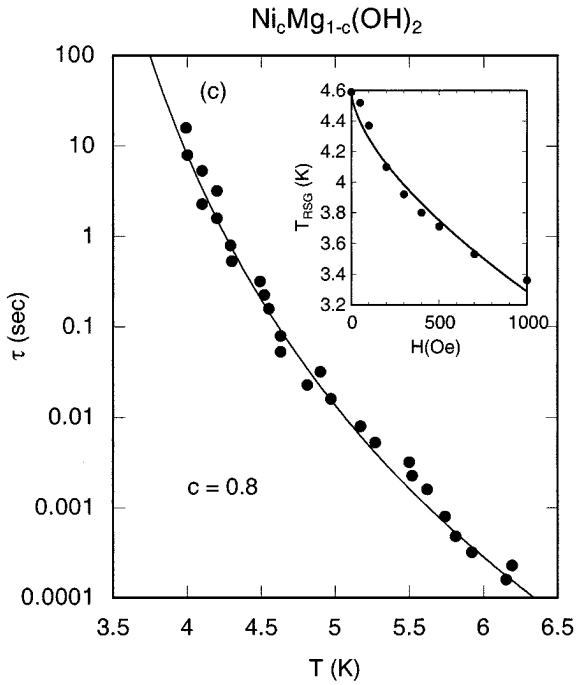

Figure 17. (Continued)

antiferromagnet a random local field is generated by a uniform magnetic field, leading to the destruction of AF long-range order. Thus the domain of the RSG phase is expanded, while the domain of the AF phase is contracted.

4.4. Origin of SG and RSG phase

We consider the origin of the SG and RSG phase in $Ni_cMg_{1-c}(OH)_2$. As shown in figure 1 there are three kinds of exchange interaction, J_1, J_2 and J_3 in $Ni(OH)_2$. The magnitudes of these interactions have been estimated in the following way by Enoki and Tsujikawa [1]. The superexchange paths of J_1, J_2 and J_3 involve one or two oxygen atoms. The interaction J_1 has the two paths of Ni–O–Ni superexchange interactions. The interaction J_2 has six equivalent paths of Ni–O–O–Ni superexchange interactions where the angles of two Ni–O–O in a path are both 98.2°. The interaction J_3 has two paths of Ni–O–O–Ni superexchange interactions, one of which has the same angle as those of J_2 and other has the angles of 98.2 and 154.2°. If the magnitudes of J_2 and J_3 are simply proportional to the number of superexchange paths ($J_2 = 3\ J_3$), the values of J_1, J_2, and J_3 can be estimated as $J_1 = 2.7$ K, $J_2 = -0.28$ K, and $J_3 = -0.09$ K by substituting the values of T_N (= 26.4 K) and the Curie–Weiss temperature Θ (= 21.6 K) into the corresponding expressions derived from the molecular field theory.

For $Ni_cMg_{1-c}(OH)_2$ with high concentration the ferromagnetic intraplanar exchange interaction J_1 is dominant over the antiferromagnetic interplanar exchange interactions J_2 and J_3. Then the system is regarded as a 2D site-random ferromagnetic system on the triangular lattice site, where the percolation threshold c_p^{2D} is expected to be 0.5 [19]. In the vicinity of $c = c_p^{2D}$ there appear Ni^{2+} spins which lose a certain number of Ni^{2+} to the nearest neighbour sites. These Ni^{2+} spins are rather strongly coupled by antiferromagnetic interplanar interactions

J_2 and J_3. The spin frustration effect arises from the competition among J_1, J_2 and J_3, leading to the SG and RSG phase. In this case the system is regarded as a 3D site-random system. The value of c_p for such a system has been roughly estimated as $c_p^{3D} \approx 2/(z_1 + z_2 + z_3) = 0.1$ by Enoki and Tsujikawa [2], where z_i is the number of nearest-neighbour spins coupled by J_i ($z_1 = 6$, $z_2 = 2$ and $z_3 = 12$). This estimated value of c_p^{3D} is in good agreement with the concentration at which T_{SG} tends to reduce to zero.

Here it is interesting to compare our data with the results of $Fe_cMg_{1-c}Cl_2$. The magnetic phase diagram of $Fe_cMg_{1-c}Cl_2$ is similar to that of $Ni_cMg_{1-c}(OH)_2$: it consists of the AF phase for $c > 0.61$, the AF and RSG phases for $0.5 < c \leqslant 0.61$ and the SG phase for $0.286 \leqslant c \leqslant 0.5$ [5, 7]. In $FeCl_2$ the intraplanar exchange interactions are ferromagnetic (J_{nn}) for the nearest neighbours, but antiferromagnetic (J_{nnn}) for the next-nearest neighbours. The origin of the SG phase and RSG phase may be due to a spin frustration effect arising from the competition between intraplanar ferromagnetic J_{nn} and antiferromagnetic J_{nnn}, in contrast to the case of $Ni_cMg_{1-c}(OH)_2$. The multicritical point where the SG, RSG and AF merge is close to the 2D percolation threshold c_p^{2D} ($= 0.5$) [19] for the triangular lattice with only J_{nn}. In the vicinity of c_p^{2D} Fe^{2+} spins are rather strongly coupled by J_{nnn}. Then the system is regarded as a 2D triangular lattice with nearest-neighbour and next-nearest-neighbour interactions. The percolation threshold of this system is predicted to be 0.295 [19]. This value is very close to the critical concentration ($= 0.286$) for the SG phase.

5. Conclusion

We have studied the magnetic phase transitions of a 3D Ising antiferromagnet with short-range interaction, $Ni_cMg_{1-c}(OH)_2$ using SQUID DC magnetization and SQUID AC magnetic susceptibility. The magnetic phase diagram consists of the SG phase for $0.1 < c < 0.5$, RSG phase for $0.5 \leqslant c \leqslant 0.8$ and AF phase for $0.5 \leqslant c \leqslant 1$. The frequency dependence of χ'' for the SG phase is different from that for the RSG phase, suggesting a difference in the origin of spin-glass behaviour. In spite of such a difference the relaxation time of the SG phase for $c = 0.25$ and the RSG phase for $c = 0.8$ obeys a conventional power-law form with the critical exponent x close to 7.9 ± 1.0 predicted for the 3D $\pm J$ short-range Ising model. This suggests that the SG phase and RSG phase are stable in thermal equilibrium below a finite freezing temperature. The RSG phase for $c = 0.5$ and 0.6 may consist of a mixed phase of spin-glass and long-range AF order. Magnetic neutron-scattering studies on single-crystal $Ni_cMg_{1-c}(OH)_2$ with $c = 0.25$, 0.5 and 0.8 are required for the further understanding of the spin-glass phase and re-entrant spin-glass phase.

Acknowledgments

The authors thank H Kawamura for valuable discussions and C R Burr for critical reading of this manuscript. This work was supported by the Research Foundation of SUNY-Binghamton (240-9807A).

References

[1] Enoki T and Tsujikawa I 1975 *J. Phys. Soc. Japan* **39** 317–23
[2] Enoki T and Tsujikawa I 1975 J. Phys. Soc. 39 324–31
[3] Enoki T and Tsujikawa I 1979 *J. Phys. Soc. Japan* **46** 1027–8
[4] Enoki T, Tsujikawa I, Hoshi A and Goto T 1978 *J. Phys. Soc. Japan* **45** 1819–26
[5] Bertrand D, Fert A R, Schmidt M C, Bensamka F and Legrand S 1982 *J. Phys. C: Solid State Phys.* **15** L883–8

[6] Gelard J, Bensamka F, Bertrand D, Fert A R, Redoules J P and Legrand S 1983 *J. Phys. C: Solid State Phys.* **16** L939–43
[7] Bertrand D, Bensamka F, Fert A R, Gelard J, Redoules J P and Legrand S 1984 *J. Phys. C: Solid State Phys.* **17** 1725–33
[8] Wong Po-zen, von Molnar S, Palstra T T M, Mydosh J A, Yoshizawa H, Shapiro S M and Ito A 1985 *Phys. Rev. Lett.* **55** 2043–6
[9] Gunnarsson K, Svedlindh P, Nordblad P, Lundgren L, Aruga H and Ito A 1988 *Phys. Rev. Lett.* **61** 754–7
[10] Gunnarsson K, Svedlindh P, Andersson J -O, Nordblad P, Lundgren L, Katori H A and Ito A 1992 *Phys. Rev.* B **46** 8227–31
[11] Suzuki I S and Suzuki M 1999 *J. Phys.: Condens. Matter* **11** 521–41
[12] Suzuki I S and Suzuki M 2000 *Mol. Cryst. Liq. Cryst.* at press
[13] Kawamura H 1998 *Phys. Rev. Lett.* **80** 5421–4
[14] de Almeida J R L and Thouless D J 1978 *J. Phys. A: Math. Gen.* **11** 983–90
[15] Kawamura H 1996 *Int. J. Mod. Phys.* **7** 345–53
[16] Ogielski A T 1985 *Phys. Rev.* B **32** 7384–98
[17] Mydosh J A 1993 *Spin Glasses: an Experimental Introduction* (London: Taylor and Francis)
[18] Fishman S and Ahalony A 1979 *J. Phys. C: Solid State Phys.* **12** L729–33
[19] Stinchcombe R B 1983 *Phase Transitions and Critical Phenomena* vol 7, ed C Domb and J L Lebowitz (London: Academic) pp 151–280